# Structure and Function Analysis of Melanocortin Analogue with Special Reference to Melanocortin Receptor Subtype

**Thesis by**

**Song-Zhe Li**

**Brain Korea 21 Project for Medical Sciences**
**The Graduate School of Yonsei University**

# Structure and Function Analysis of Melanocortin Analogue with Special Reference to Melanocortin Receptor Subtype

**Directed by Professor Sung-Kil Lim**

**A Dissertation Submitted to the Faculty**

**of The Graduate School of Yonsei University**

**December, 2000**

**Thesis by**

**Song-Zhe Li**

**Brain Korea 21 Project for Medical Sciences**
**The Graduate School of Yonsei University**

**A Dissertation for the Doctoral Degree of Philosophy by Song-Zhe Li has been approved by**

_____

**Supervisory Committee, Chairman**

_____

**Supervisory Committee**

_____

**Supervisory Committee**

_____

**Supervisory Committee**

_____

**Supervisory Committee**

**Brain Korea 21 Project for Medical Sciences**
**The Graduate School of Yonsei University**

**December, 2000**

# Acknowledgements

I would like to express my sincere appreciation for the direction of Professor Sung-Kil Lim. And I greatly appreciate Professor Kap-Bum Huh, Associate Professor Min-Gul Lee, Research Assistant Professor Ja-Hyun Baik, and Research Assistant Professor Kwang-Chul Chung for their kind helps in this thesis. I am also deeply grateful to Professor Wontae Lee and the members in his laboratory (Department of Biochemistry, College of Science, Yonsei University) for their kind assistance. In addition, I thank Dr. Roger. D. Cone (Vollum Institute for Advance Biomedical Research, Portland, OR, USA) for kindly supplying the rMC3R and hMC4R cDNA and thank Dr. Ira Gantz (Department of Surgery, University of Michigan Medical Center, Ann Arbor, MI, USA) for kindly supplying the hMC1R cDNA. In this study, I also received kind help from the colleagues in our laboratory, as well as the other research assistants and the officers in our Medical Research Center.

# Contents

# List of Figures

# List of Tables

## ABSTRACT

# Structure and function analysis of melanocortin analogue with special reference to melanocortin receptor subtype


## Song-Zhe Li

*Brain Korea 21 Project for Medical Sciences*
*The Graduate School of Yonsei University*

**(Directed by Professor Sung-Kil Lim)**



Melanocortins, including α-MSH have been implicated in a variety of physiologic functions, such as skin pigmentation, learning, memory, analgesic and anti-inflammatory effects, the regulation of blood pressure, immune modulation and food intake. The cloning of five melanocortin receptor subtypes provided the tools for the systemic study of the molecular mechanisms involved their physiologic effects. As melanocortin reveals many different effects through the distinct receptor subtype, a selective ligand for a given receptor subtype is required to reduce the undesirable effects of melanocortin, accordingly, the structure and function analysis of ligand-receptor interactions has become more important. To search for new melanocortin analogues with high potency and selectivity for a given melanocortin receptor subtype, understand the more detailed characteristics of ligand-receptor interaction, and if possible, to develop candidate compounds likely to be used as anti-obesity drugs, we synthesized α-MSH analogues and compared their biological activity, including binding and cAMP-generating activity in CHO cell lines over-expressing hMC1R, rMC3R or hMC4R, and investigated their NMR structures and their patterns of ligand-receptor interaction to each receptor subtype by homology modeling analysis. Compared to [Nle$^4$]α-MSH, the linear MTII (melanotan II) designated as α-MSH-ND, in spite of deletion of several N- and C-terminal residues, exhibited better activity at both the MC3R and MC4R, while its $IC_{50}$ and $EC_{50}$ values were comparable to those of MTII reported previously. [Nle$^4$]α-MSH showed a loop structure, while α-MSH-ND revealing a tight type I β-turn conformation.

Substitution of the $His^6$ residue of α-MSH-ND by Gln, Trp, Asn, Arg, Lys or Tyr, with the exception of [$Arg^6$]α-MSH-ND, most of the α-MSH-ND analogues revealed lower activity than α-MSH-ND at all three receptors. Among the several analogues examined, [$Gln^6$]α-MSH-ND had about 10,000 times less biological activity than α-MSH-ND at MC1R, whereas, the potencies of both oligopeptides were comparable at MC3R or MC4R. [$Gln^6$]α-MSH-ND exhibited a type I' β-turn that was very similar to the type I β-turn structure of α-MSH-ND, but a remarkable structural difference was observed at the side chain orientations of the $6^{th}$ and $7^{th}$ residues of [$Gln^6$]α-MSH-ND, which were mirror images of those of α-MSH-ND. By homology modeling analysis, $His^6$ of α-MSH-ND was found to interact with the TM2 regions of all three receptors ($Glu^{94}$ of MC1R, $Glu^{94}$ of MC3R, and $Glu^{100}$ of MC4R), but [$Gln^6$]α-MSH-ND did not. The phenyl ring of the D-$Phe^7$ residue of [$Gln^6$]α-MSH-ND revealed interaction with the TM3 regions of MC3R and MC4R ($Ser^{122}$ of MC3R or $Ser^{127}$ of MC4R). In MC1R, however, these serine residues corresponded to $Val^{122}$, which contains two methyl groups that induce steric hindrance with D-$Phe^7$ of [$Gln^6$]α-MSH-ND. This might explain why the biological activity of [$Gln^6$]α-MSH-ND at MC1R was significantly lower than that at MC3R or MC4R. In the *in vivo* experiments, it was found that intraperitoneal injection of α-MSH-ND (100nmole) gave rise to a significant inhibition of food intake for up to 3 hours ($P<0.05$ or $P<0.01$). These results suggest that a type I β-turn conformation comprising the residues of $Asp^5$-$His^6$-(D-$Phe$)$^7$-$Arg^8$ is important, especially, the side chain orientations of $6^{th}$ and $7^{th}$ residues is critical for determination of potency and selectivity of melanocortin analogues. MC1R-reluctance with the preservation of comparable MC3R and MC4R selectivity could be achieved by modifying the D-$Phe^7$ orientation of α-MSH-ND, while keeping the 'type I β-turn'-like structure. In addition, α-MSH-ND and its derivatives, especially those with high biological activity at MC3R and/or MC4R, could directly inhibit food intake.

**Key Words:** melanocortin receptor; binding affinity; cAMP-generating activity; NMR; type I β-turn; homology modeling.

# Structure and function analysis of melanocortin analogue with special reference to melanocortin receptor subtype

**Song-Zhe Li**

***Brain Korea 21 Project for Medical Sciences***
***The Graduate School of Yonsei University***

**(Directed by Professor Sung-Kil Lim)**

## I. INTRODUCTION

The peptide hormone precursor pro-opiomelanocortin (POMC) is post-translationally cleaved to give rise to a variety of biologically active substances called melanocortic peptides (melanocortins), including α-, β-, and γ-melanocyte stimulating hormones (MSH) and adrenocorticotropin[1]. Melanocortins are primarily known to for their role in the regulation of skin pigmentation[2], adrenal steroid production[3]. They also induce wide array of physiological effects. For example, the melanocortins have been shown to affect memory, behavior, inflammation, pyretic control, analgesia, blood pressure, nerve growth and regeneration and weight homeostasis, and to influence events surrounding parturition[4-9]. The cloning of five different melanocortin receptors (MC1R-MC5R)[10-14] during the years 1992-1994 started a new era in the research on the melanocortin receptors and provided tools for systematic studies of the molecular mechanisms exerting the above effects.

The melanocortin receptors show distinct distributions in the body[15,16]. The melnocortin MC1 receptor (MC1R) was first recognized as the peripheral MSH receptor which is present in the melnocytes, where it regulates the pigmentation of the skin in a variety of vertebrates[17]. More recently, it has become known that the MC1R is present in many cell types, including the periphery and CNS system, such as melanoma cells[18], macrophage and monocytes[19,20], neutrophils[21], endothelial cells[20], glioma cell and astrocytes[22], fibroblasts[23] and keratinocyte [24]. The melanocortin MC2 receptor (MC2R) was recognized as the ACTH

receptor and participates in the regulation of steroid production in the adrenal gland. The melanocortin MC3 receptor (MC3R) is found in the brain, and in placenta, gut and heart tissue[12,25,26]. The MC4 receptors (MC4R) has only been found in the CNS, where it is expressed at distinct loci, including the cortex, thalamus, hypothalamus, brain stem and spinal cord[13,27]. The melanocortin MC5 receptor (MC5R) was found to have a wide distribution in the body. Although the MC4R expression was not detectable in the periphery in detailed studies covering 20 human organs[26], the MC4R was expressed in many peripheral tissues of the chicken[28].

POMC gene expression is limited to ARC (arcuate) neurons that project to areas that express melanocortin receptors and participate in energy homeostasis. Since leptin receptors are expressed on POMC neurons, melanocortin neurons appear to be a target of leptin action[29,30]. MC3R and MC4R, unlike the other subtypes, were found mainly at distinct loci in the central nervous system, especially, the ventromedial nucleus of the hypothalamus (VMH) which is considered most important in the regulation of feeding[25]. Mutations of the POMC gene in humans[31] or the MC4R gene in mice[32] have resulted in obesity, while the overexpression of agouti or agouti-related protein has also induced obesity in mice[33]. Activation of the MC4R by α-MSH increases the energy expenditure, decreases the food intake, and promotes sympathetic activity[6]. Recently, Chen et al found that MC3R-knockout mice have increased fat mass, reduced lean mass and higher feed efficiency and demonstrated that MC3R also serves non-redundant roles similar to MC4R in the regulation of energy homeostasis[34]. These findings, directly or indirectly, provided the evidences that melanocortin is involved critically in the control of food intake and body weight homeostasis via MC3R and MC4R. Therefore, MC3R- and/or MC4R-selective substances have been listed as important one of the candidates in development of anti-obesity drugs.

The natural melanocortic peptides (α-MSH, β-MSH, γ-MSH and ACTH) do not clearly discriminate between the different melanocortin receptor subtypes, with the exception that α-MSH is selective for the MC1R and ACTH for the

MC2R. A very useful linear peptide is [Nle$^4$, D-Phe$^7$]α-MSH (Melanotan-I, NDP-MSH) as it shows high affinity for the melanocortin receptors, and as it can be labeled with iodine and used as radioligand. However, most (if not all) of these linear or cyclic peptides (at least as far as they have been tested) seem not to deviate from the potency order MC1R > MC3R > MC4R > MC5R. Melanotan-II(MTII) is a cyclic MSH analogue synthesized quite long time ago[35]. It has recently been used in various functional studies as a non-selective MC3R/MC4R agonist, whereas it is still quite potent at MC1R[16]. Subsequently, Hruby et al. synthesized a cyclic lactam peptide, SHU9119, which was claimed to show selectivity and antagonistic activity at MC4R[36]. However, Schiöth et al. found that the compound to be essentially non-selective for the melanocortin receptor subtypes[37]. Thus the usefulness of SHU9119 as an experimental tool for melanocortin receptor subtype classification seems to be limited[16]. Until now, most α-MSH analogues have preferably bound to the MC1R, MC3R and the MC4R with high affinity. Development of melanocortin receptor antagonist and selective melanocortin receptor active compounds especially for the MC3R and MC4R is still an important task.

NDP-MSH with a seven-lactam-ring structure has been known as the most potent melanocortin agonist[38]. The substitution of Phe$^7$ in α-MSH to D-Phe$^7$ increased the receptor-binding and cAMP response, providing the insight that the core structure of α-MSH analogues is critically important for ligand-receptor interaction and selectivity[39]. To search for new melanocortin analogues with high potency and selectivity for a given melanocortin receptor subtype, understand the more detailed characteristics of ligand-receptor interaction, and if possible, to develop candidate compounds likely to be used as anti-obesity drugs, we synthesized several new α-MSH analogues with D-Phe at the 7$^{th}$ position and tested their biological activity in CHO cell lines stably transfected with hMC1R, rMC3R or hMC4R, and their conformational features with NMR spectroscopy. Furthermore, we evaluated the ligand-binding traits of the three melanocortin receptor subtypes with homology modeling analysis. Finally, the synthetic

melanocortin analogue with the highest biological activity at MC3R and MC4R was tested *in vivo* to evaluate if it has an inhibitory effect on food intake.

# II. MATERIALS AND METHODS

## 1. Chemicals

All media and sera for cell cultivation were purchased from Gibco-BRL (U.S.A.). NDP-MSH and other chemicals were purchased from Sigma (U.S.A.) unless specified otherwise.

## 2. Preparation of a -MSH analogues

The peptides used in this study (except NDP-MSH) were synthesized at the Korea Basic Science Institute (Seoul, Korea) by use of the solid phase approach and purified by high performance liquid chromatography (HPLC). The peptide sequences were assembled with a Milligen 9050(Fmoc Chemistry). The correct molecular weights of the peptides were confirmed by mass spectrometry. For deprotection, a reagent mixture (88% trifluoroacetic acid, 5% phenol, 2% triisopropylsilane, 5% $H_2O$; 2 hours) was used. The raw peptides formed were purified by HPLC (Delta PAK 15μ C18 300Å3.9mm×150mm column, detection at 240nm).

## 3. Sub-cloning of melanocortin receptor cDNAs into mammalian expression vector

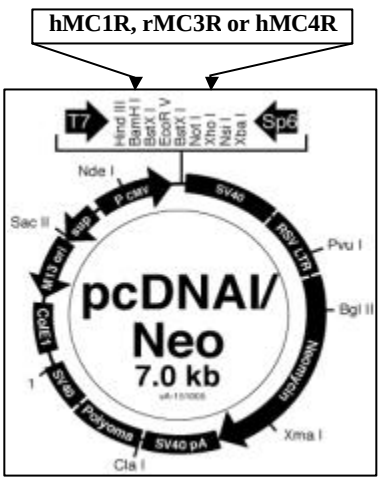


The hMC1R, rMC3R and hMC4R cDNAs in were kindly provided as gifts by Dr. Gantz, I. (Department of Surgery, Univers-ity of Michigan Medical Center, Ann Arbor, MI, USA) and Dr. Cone R.D. (Vollum Institute for Advance Biomedical Research, Portland, OR, USA), respectively. For stable

**Figure 1**. Subcloning of hMC1R, rMC3R and hMC4R into pcDNA I/neo vector at the restriction enzyme sites of BamH I and Xho I, respectively.

transfection, each of these cDNAs was sub-cloned into the mammalian expression vector pcDNA I/neo at the multi-cloning site, BamH I and Xho I, as shown in Figure 1. And enough recombinant plasmid DNAs were prepared with the Plasmid Purification Kit (Cat. No. 12143, QIAGEN GmbH, Germany).

**4. Preparation of mammalian cell lines stably expressing the melanocortin receptor subtypes**

CHO cells were maintained in a F-12 medium (with glutamine) supplemented with 10% fetal bovine serum, 100 units/ml penicillin G sodium, 100 μg/ml streptomycin sulfate and 0.25 μg/ml amphotericin B. Cells were incubated in a 100-mm culture dish at 37 °C in humidified air containing 5% $CO_2$. For transfections, the hMC1R, rMC3R and hMC4R cDNAs were cloned into the expression vector pcDNA I/neo. Cells were generally at 50% confluence on the day of transfection, which was carried out using the calcium phosphate method, as described previously[40]. Briefly, cells were fed with fresh complete culture medium containing 20 mM HEPES and incubated in 95% air/5% $CO_2$. After 3-4 hours, the medium was discarded and 5 ml of calcium phosphate-DNA precipitate containing 25 μg DNA, 124 mM $CaCl_2$, 140 mM NaCl, 25 mM HEPES and 1.41 mM $Na_2HPO_4$ (pH 7.12) was added. The cells were then incubated for 4 hours with 97% air/3% $CO_2$, washed with phosphate buffered saline (PBS, 137 mM NaCl, 2.68 mM KCl, 4.3 mM $N_2HPO_4$, and 1.47 mM $KH_2PO_4$, at pH 7.12), and shocked with glycerol buffer (15% glycerol, 140 mM NaCl, 25 mM HEPES and 1.41 mM $Na_2HPO_4$, at pH 7.12). Cells were washed again with PBS, and incubated for an additional 36-48 hours in complete F-12 medium. Cells were then cultured in complete F-12 medium containing 0.5 mg/ml G418 (Geneticin; Life Technologies) until G418-resistant colonies were generated. G418-resistant colonies were picked out and then sub-cultured for at least 10-14 days. Finally, hMC1R-, rMC3R- and hMC4R-expressing cells were identified by screening more than 15 colonies and confirmed by assaying NDP-MSH-induced cyclic AMP accumulation.

**5. Binding assay**

Iodinated NDP-MSH, $^{125}$I(Iodotyrosyl$^2$)-[Nle$^4$, D-Phe$^7$]α-MSH, was prepared

by the modified chloramine-T method, as described previously[40]. 1 mCi(10 µl) of $Na^{125}I$ (Amersham) was added to 5 µg of NDP-MSH in 100 µl of 200 mM sodium phosphate buffer (pH 7.2). 20 µl of 2.8 mg/ml chloramine T solution in 200 mM sodium phosphate (pH 7.2) was then added and allowed to stand for 15 seconds, 50 µl of 3.6 mg/ml sodium metabisulfate was then added to stop the reaction. The reaction mixture was diluted with 1 ml of 0.1% BSA solution containing 0.1% trifluoroacetic acid and purified using a C18 Sep-Park cartridge (Waters) and by Sephadex G25 Gel Filtration Chromatography. The purified reagents were collected in 0.5 ml aliquots in Sigmacote-coated sterile glass tubes, into which 100 µl of PBS buffer containing 0.1% bovine serum albumin had been added in advance. For binding assays, the stably transfected CHO cells were plated 48 hours before experiments in 24-well culture plates (Falcon Plastics) at a density of $5\times10^4$ per well until they were 90-95% confluent on the day of the assay. Maintenance media was removed and the cells were washed twice with washing buffer (50 mM Tris, 100 mM NaCl, 5 mM KCl, and 2 mM $CaCl_2$, at pH 7.2), and then immediately incubated at 37°C for 2 hours with 0.25ml binding buffer per well (50 mM Tris, 100 mM NaCl, 5 mM KCl, 2 mM $CaCl_2$, 5% Hanks' Balanced Salt Solution, and 0.5% Bovine Serum Albumin, at pH 7.2) containing a constant concentration of [$^{125}$I]NDP-MSH and appropriate concentrations of the unlabeled competing ligand. After incubation, the plates were placed on ice for 15min, washed twice with 0.5 ml of ice-cold binding buffer, and detached from the plates using 0.5 ml of 50 mM NaOH twice (final volume: 1ml). Radioactivity was then determined (Workman automatic gamma counter) and data analyzed with a software package suitable for radioligand binding data analysis (GraphPad Prism Program). Nonspecific binding was determined by measuring the amount of bound [$^{125}$I]NDP-MSH remaining in the presence of $10^{-5}$ M unlabeled NDP-MSH, while specific binding was calculated by subtracting the nonspecifically bound radioactivity from total bound radioactivity. $IC_{50}$ (nM) values were reported as mean ± SE. All of the binding assays were performed in triplicate wells and repeated twice.

**6. Cyclic AMP assay**

Intracellular cyclic AMP levels were determined using the method described previously[40]. CHO cells over-expressing MC1R, MC3R or MC4R were grown to 90-95% confluence in 24-well plates. Cell culture media was exchanged with complete F-12 medium containing 10% fetal bovine serum 3-4 hours, before cells were treated with peptides. For assays, the media was removed and cells washed with 0.5 ml of cAMP-generating medium (10% fetal bovine serum, 2 mM IBMX, 0.1% bovine serum albumin, 20 mM HEPES, and 0.002% ascorbic acid in F-12 Medium). 0.25 ml of cAMP-generating media containing various concentrations of peptides was added and cells were incubated for 30 min at 37 °C. At the end of this incubation, media was completely discarded, and cells were frozen at –70 °C for 30 minutes and thawed at room temperature for 15-20 minutes. This freezing-thawing process was then repeated twice. Cells were detached from the plates with 1ml of 50 mM HCl solution per well, transferred to a 1.5-ml Eppendorf tube, and centrifuged at 1900×g for 10 min. The supernatants were diluted 50-fold with acetate buffer and cAMP concentrations were measured using a cAMP $^{125}$I RIA Kit (Diasorin, USA), according to the assay instructions. The mean values of the data so collected were fitted to a sigmoid curve with a variable slope factor by non-linear regression in a GraphPad Prism. $EC_{50}$ (nM) values are described as mean ± SE. All of the cAMP assays were performed in triplicate wells and repeated twice.

**7. Solution structure analysis with NMR methods**

Five α-MSH analogues, including [Nle$^4$]α-MSH, α-MSH-ND, [Gln$^6$]α-MSH-ND, [Gln$^6$]α-MSH-ND(6-10) and [Lys$^6$]α-MSH-ND were dissolved in 90% $H_2O$/10% $D_2O$ or 99.99% $D_2O$ at pH value of 7.0 with 50mM sodium phosphate buffer. NMR samples with $D_2O$ were prepared after lyophilization of an $H_2O$ sample. The final sample concentrations for NMR measurements were 2mM in 0.5mL buffer solution.

NMR experiments were carried out at 10 °C on a Bruker DRX-500 spectrometer equipped with a triple resonance probe having x,y,z gradient coils.

NMR spectra were recorded at 10 °C. Two-dimensional total correlation spectroscopy (TOCSY)[41] and two-dimensional nuclear Overhauser effect spectroscopy (NOESY)[42] were performed. Two-dimensional rotating-frame Overhauser effect spectroscopy (ROESY) spectra were also recorded in $D_2O$ solution. Two-dimensional double-quantum-filtered (DQF) COSY spectra[43] were collected in $H_2O$ to obtain a vicinal coupling constant. A series of one-dimensional NMR measurements were accomplished to identify slowly exchanging amide hydrogen resonance on a freshly prepared $D_2O$ solution after lyophilization of a $H_2O$ sample. All NMR experiments were performed in the phase-sensitive mode using the time proportional phase incrementation (TPPI) [44,45]. All NMR data were processed using nmrPipe/nmrDraw (Biosym/Molecular Simulations, Inc.) or XWIN-NMR (Bruker Instruments) software. Processed data were analyzed using Sparky 3.60 developed at UCSF on a Silicon Graphics Indigo$^2$ workstation

Finally, the hybrid distance geometry and dynamical simulated-annealing protocol with the X-PLOR 3.81 program on a Silicon Graphics Indigo$^2$ workstation were used for structure calculations. Distance geometry (DG) substructures were generated using a subset of atoms and followed a refinement protocol described by Lee et al[46]. The target function for molecular dynamics (MD) and energy minimization (EM) consisted of covalent structure, van der Waals repulsion, NOE and torsion angle constraints.

**8. Homology modeling analysis of receptor subtypes**

Transmembrane regions of receptor molecules were determined from both sequence alignment and topology prediction data of hMC1R, rMC3R and hMC4R[47]. The primary sequence alignment data were obtained from Haskell-Luevane et al[48]. The molecular topology prediction of receptors was performed by Tosts method on EMBL protein-predict server and these data were aligned with bovine rhodopsin sequence. The helical segments were constructed using bovine rhodopsin coordinates previously reported[49] and further refined by energy minimization procedure. The force field used for modeling calculations

was cvff in Discover Module of InsightII program (MSI Inc.) on SGI Indigo$^2$ workstation. Three-dimensional structures of receptor molecules were completed by replacement of helical segments of the bovine rhodopsin onto melanocortin receptor sequences, followed by rearrangements of helix orientations based on mutagenesis data of receptor molecules[50]. The previous mutagenesis and biochemical data also provided information about the relative side chain orientations of amino acids in receptor molecule[51]. The receptor-ligand complex structures form MC1R, MC3R and MC4R were finally generated by ligand docking procedure based on mutagenesis and NMR data.

**9. Feeding assay**

(1) Animals: 25~30 g male ICR mice were used for feeding assay. Mice were maintained on a normal 12h/12h light/dark cycle with food and water *ad libitum* before experiments.

(2) In vivo experiments: Before injection, animals were housed in metabolic cages individually for at least 24 h, and then fasted with food deprivation from 18:00 to 8:00 to stimulate feeding during the daytime experimental period. They were distributed into weight-matched control and experimental groups with 9 mice/group, and injected intraperitoneally with vehicle (saline, 100 μl each mouse) and vehicle plus drug (α-MSH-ND, 100 nmole/100 μl in saline) as indicated. Twelve-hour of feeding assay was performed. Briefly, the quantity of food pellets in spill-free cup was pre-measured. Food remaining was removed and weighted at the time internals indicated. Significance of drug effect at individual time points was determined by two-way ANOVA.

# III. RESULTS

We designed and synthesized a series of new linear melanocortin analogues in which the structures are aligned with [Nle$^4$]α-MSH (Table 1). The hMC1R, rMC3R and hMC4R DNAs were stably and independently expressed in CHO cells for competitive receptor binding with [$^{125}$I]NDP-MSH as a radioligand and a cyclic AMP accumulation test following treatment with different ligands.

**Table 1. Amino acid sequences of a-MSH analogues designed and tested in this study.** All peptides have an acetyl-group on the N terminus and an amide group on the C terminus. The main substituted amino acid residues are shown in Italics

| Peptides | Position | | | | | | | | | | | | |
|---|---|---|---|---|---|---|---|---|---|---|---|---|---|
| | 1 | 2 | 3 | 4 | 5 | 6 | 7 | 8 | 9 | 10 | 11 | 12 | 13 |
| [Nle$^4$]α-MSH | Ser | Tyr | Ser | Nle | Glu | His | Phe | Arg | Trp | Gly | Lys | Pro | Val |
| α-MSH-ND | | | | Nle | Asp | His | D-Phe | Arg | Trp | Lys | | | |
| [Gln$^6$]α-MSH-ND | | | | Nle | Asp | *Gln* | D-Phe | Arg | Trp | Lys | | | |
| [Asn$^6$]α-MSH-ND | | | | Nle | Asp | *Asn* | D-Phe | Arg | Trp | Lys | | | |
| [Tyr$^6$]α-MSH-ND | | | | Nle | Asp | *Tyr* | D-Phe | Arg | Trp | Lys | | | |
| [Trp$^6$]α-MSH-ND | | | | Nle | Asp | *Trp* | D-Phe | Arg | Trp | Lys | | | |
| [Arg$^6$]α-MSH-ND | | | | Nle | Asp | *Arg* | D-Phe | Arg | Trp | Lys | | | |
| [Lys$^6$]α-MSH-ND | | | | Nle | Asp | *Lys* | D-Phe | Arg | Trp | Lys | | | |
| α-MSH-ND(6-10) | | | | | | His | D-Phe | Arg | Trp | Lys | | | |
| [Gln$^6$]α-MSH-ND(6-10) | | | | | | *Gln* | D-Phe | Arg | Trp | Lys | | | |
| [Asn$^6$]α-MSH-ND(6-10) | | | | | | *Asn* | D-Phe | Arg | Trp | Lys | | | |
| [Trp$^6$]α-MSH-ND(6-10) | | | | | | *Trp* | D-Phe | Arg | Trp | Lys | | | |

## 1. Preparation of CHO cell lines stably expressing the different MC receptor subtypes

With stabe transfection by the calcium phosphate method, the cell lines which were G418-resistant were selected by assay of NDP-MSH-induced cyclic AMP accumulation. As shown in Figure 2, compared to the vehicle-treated group,

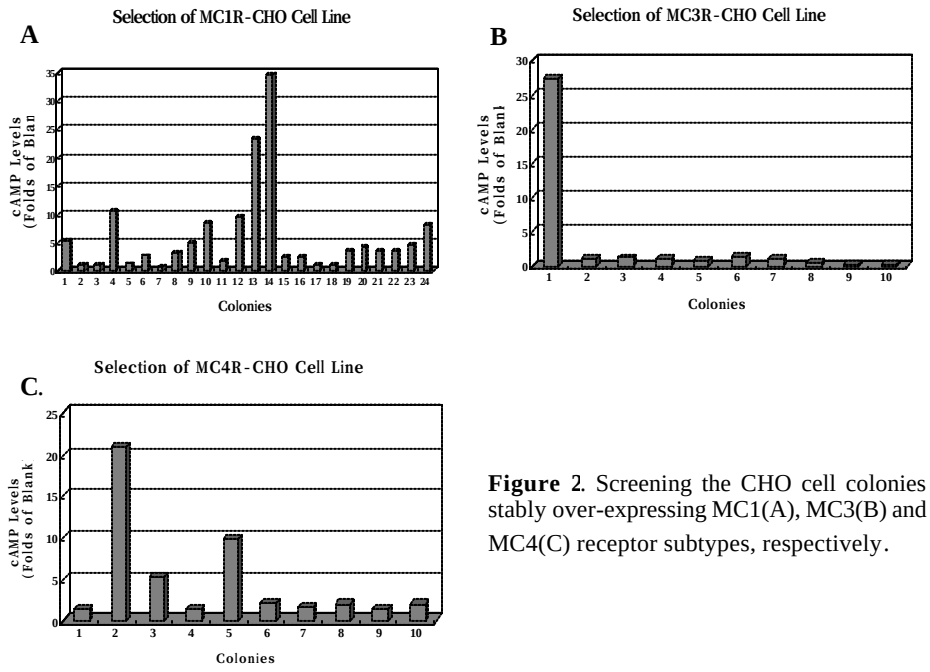


**Figure 2.** Screening the CHO cell colonies stably over-expressing MC1(A), MC3(B) and MC4(C) receptor subtypes, respectively.

the 14th cell colony in MC1R, the 1st cell colony in MC3R and the 2nd cell colony in MC4R, exhibited the most significant increase of intracellular cAMP levels, respectively. The three cell lines were then used for subsequent experiments for evaluating the biological activity of α-MSH analogues.

## 2. Comparative analysis of binding activity

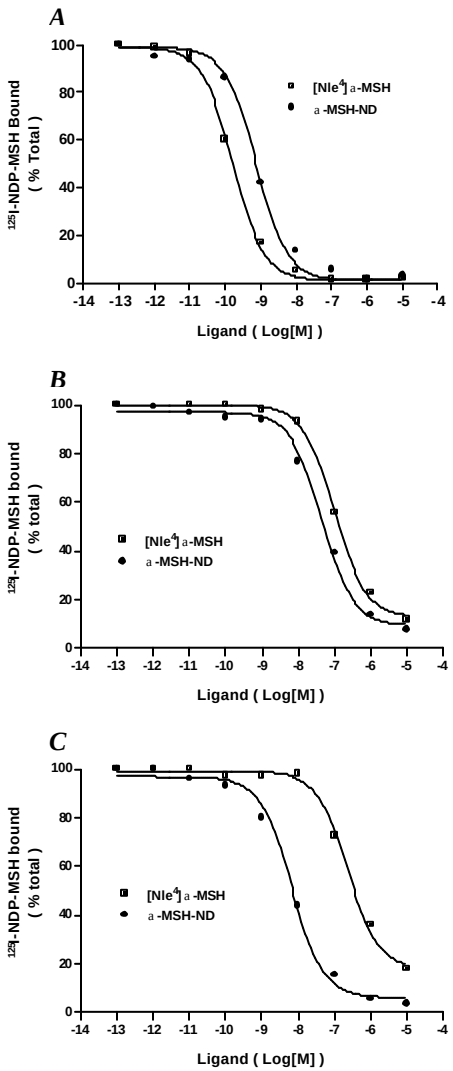


**Figure 3**. Competition curves of α-MSH analogues ([Nle$^4$] α-MSH and α-MSH-ND) obtained in CHO cell lines stably transfected with MC1R( **A**), MC3R(**B**) and MC4R(**C**) using a fixed concentration of [$^{125}$I]NDP-MSH and varying concentrations of the unlabeled competing peptides. Each experiment was performed in triplicate and repeated twice.

As seen in Figure 3A, for MC1R, the preferential order was shown with [Nle$^4$]α-MSH > α-MSH-ND. Their $IC_{50}$ values (nM) at MC1R were 0.166±0.028 and 0.769±0.486 (as seen in Table 2). For MC3R, the preferential order was shown as α-MSH-ND > [Nle$^4$]α-MSH, and for MC4R, the same preferential order was obtained (Figure 3B and 3C). Compared with their binding affinity for MC3R and MC4R, the two analogues revealed the preference to MC1R. In particular, substitution of the 7th residue from Phe to D-Phe induced the remarkably potentiated selectivity for MC4R. Although without the N-terminal three amino acid residues, α-MSH-ND still revealed a higher binding affinity than [Nle$^4$]α-MSH to MC3R and MC4R.

With the His$^6$ residue of α-MSH-ND being substituted by Gln, Trp, Asn, Arg, Lys or Tyr, except [Arg$^6$]α-MSH-ND, the other analogues gave significantly decreased binding affinities for

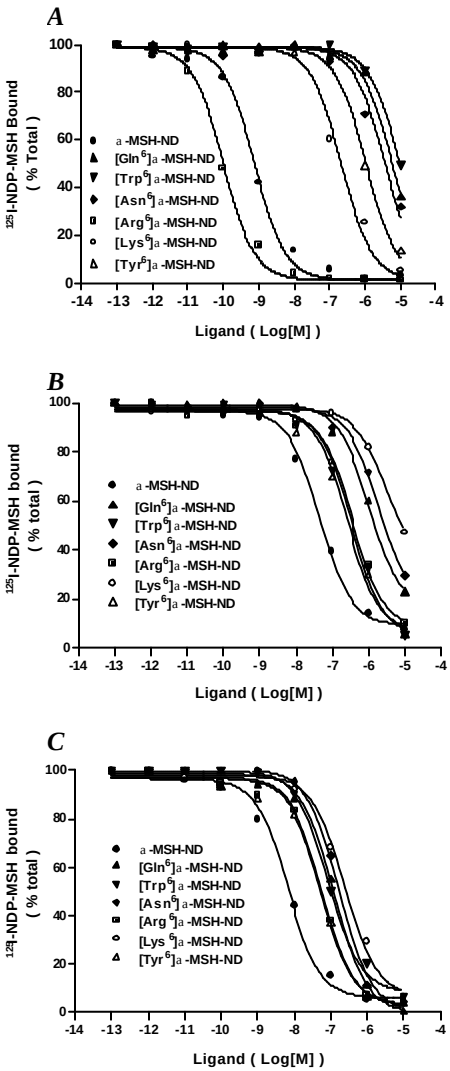


**Figure 4**. Competition curves of α-MSH analogues (α-MSH-ND, [Gln$^6$]α-MSH-ND, [Trp$^6$]α-MSH-ND, [Asn$^6$]α-MSH-ND, [Arg$^6$]α-MSH-ND, [Lys$^6$]α-MSH-ND and [Tyr$^6$]α-MSH-ND) obtained in CHO cell lines stably transfected with MC1R(**A**), MC3R(**B**) and MC4R(**C**) using a fixed concentration of [$^{125}$I]NDP-MSH and varying concentrations of the unlabeled competing peptides. Each experiment was performed in triplicate and repeated twice.

MSH-ND > [Tyr$^6$]α-MSH-ND > [Asn$^6$]α-MSH-ND > [Gln$^6$]α-MSH-ND > [Trp$^6$]α-MSH-ND. For MC3R and MC4R, all of the substitutes MC1R (Figure 4A). Their MC1R-binding affinity exhibited the different preference in the order of [Arg$^6$]α-MSH-ND > α-MSH-ND >> [Lys$^6$]α-

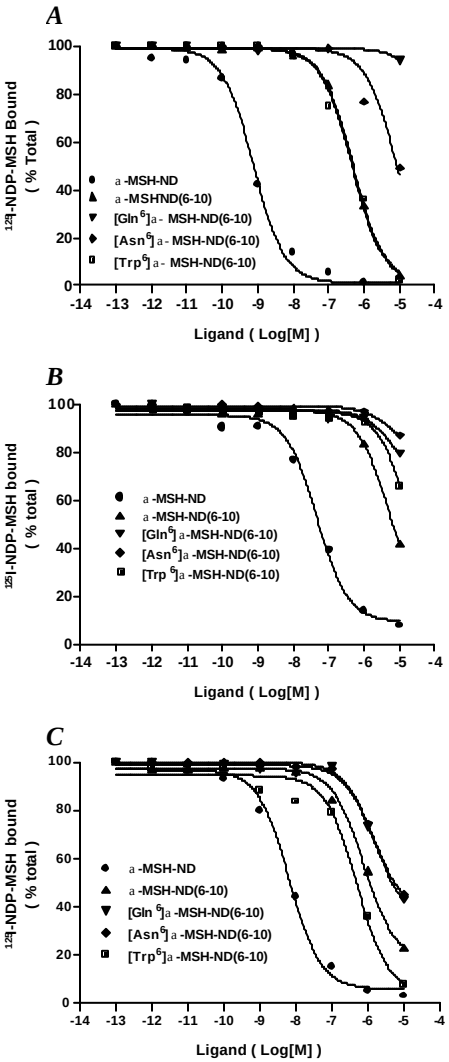


**Figure 5**. Competition curves of α-MSH analogues (α-MSH-ND, α-MSH-ND(6-10), [Gln$^6$]α-MSH-ND(6-10), [Asn$^6$]α-MSH-ND(6-10) and [Trp$^6$]α-MSH-ND(6-10) ) obtained in CHO cell lines stably transfected with MC1R(**A**), MC3R(**B**) and MC4R(**C**) using a fixed concentration of $^{125}$I]NDP-MSH and varying concentrations of the unlabeled competing peptides. Each experiment was performed in triplicate and repeated twice.

showed decreased binding affinities for both receptors (Figure 4B and 4C). Their MC3R-binding activity exhibited a different preference in the order α-MSH-ND > [Tyr$^6$]α-MSH-ND > [Trp$^6$]α-MSH-ND > [Arg$^6$]α-MSH-ND > [Gln$^6$]α-MSH-ND > [Asn$^6$]α-MSH-ND > [Lys$^6$]α-MSH-ND with their $IC_{50}$ values (nM) being 47.2±9.08, 219.3±31.585, 346.4±70.13, 361.5±57.73, 1074.0±120.01, 1998.0±363.34, 3340.0±877.05, respectively (Table 2). For MC4R, their preferential order was similar to that observed in MC3R, being α-MSH-ND > [Tyr$^6$]α-MSH-ND > [Arg$^6$]α-MSH-ND > [Trp$^6$]α-MSH-ND > [Gln$^6$]α-MSH-ND > [Asn$^6$]α-MSH-ND > [Lys$^6$]α-MSH-ND. By comparing their binding affinity to the three receptors, it could be found that, except Arg, replacements of His$^6$ with the other residues resulted in about 10,000 folds decrease in receptor-binding affinities for MC1R, while still keeping certain binding activities at MC3R and MC4R. With respect to [Gln$^6$]α-MSH-ND, as shown in Figure 4, its binding affinity were greatly weakened relative to α-MSH-ND for MC1R compared those for MC3R and MC4R.

**Table 2**. $IC_{50}$ Values (mean±SEM) of α-MSH analogues obtained from computer analysis of competition curves on stable transfected CHO Cells over-expressing MC1R, MC3R or MC4R

| Ligands | $IC_{50}$(nM) | | |
|---|---|---|---|
| | MC1R | MC3R | MC4R |
| [Nle$^4$]α-MSH | 0.166 ± 0.028 | 106.7 ± 32.25 | 238.3 ± 30.47 |
| α-MSH-ND | 0.769 ± 0.486 | 47.2 ± 9.08 | 6.7 ± 1.07 |
| [Gln$^6$]α-MSH-ND | 5962.0 ± 730.9 | 1074.0 ± 120.01 | 112.0 ± 25.94 |
| [Trp$^6$]α-MSH-ND | 9605.0 ± 4060.0 | 346.4 ± 70.13 | 87.6 ± 30.47 |
| [Asn$^6$]α-MSH-ND | 3709.0 ± 509.21 | 1998.0 ± 363.34 | 171. 2 ± 14.81 |
| [Arg$^6$]α-MSH-ND | 0.101 ± 0.035 | 361.5 ± 57.73 | 57.4 ± 8.37 |
| [Lys$^6$]α-MSH-ND | 216.30 ± 82.363 | 3340.0 ± 877.05 | 238.1 ± 40.63 |
| [Tyr$^6$]α-MSH-ND | 1075.00 ± 408.654 | 219.30 ± 31.585 | 54.860 ± 10.580 |
| α-MSH-ND(6-10) | 501.700 ± 96.770 | 4730.0 ± 1180.93 | 827.0 ± 208.73 |
| [Gln$^6$]α-MSH-ND(6-10) | 156700 ± 22148 | 7156.0 ± 5063.46 | 1297.0 ± 392.28 |
| [Asn$^6$]α-MSH-ND(6-10) | 8070.00 ± 2087.26 | 6712.0 ± 4169.22 | 1304.0 ± 378.47 |
| [Trp$^6$]α-MSH-ND(6-10) | 490.90 ± 109.59 | 23220 ± 18996 | 603.5 ± 163.9 |

The truncated peptides revealed lower affinities generally for the three receptors (Figure 5). For MC1R, the order of their binding affinity was [Trp$^6$]α-

MSH-ND(6-10) ≈ α-MSH-ND(6-10) > [Asn$^6$]α-MSH-ND(6-10) >> [Gln$^6$]α-MSH-ND(6-10). And in MC3R, the $IC_{50}$ values (nM) were 23,22±18,996, 4730 ±1180, 6712.0±4169.22, 7156.0±5063.46, while 603.5±163.9, 1297.0±392.28, 1304.0±378.47 and 827.0±208.73 for the MC4R, respectively (Table 2).

### 3. Effects of the synthesized peptides on cyclic AMP accumulation

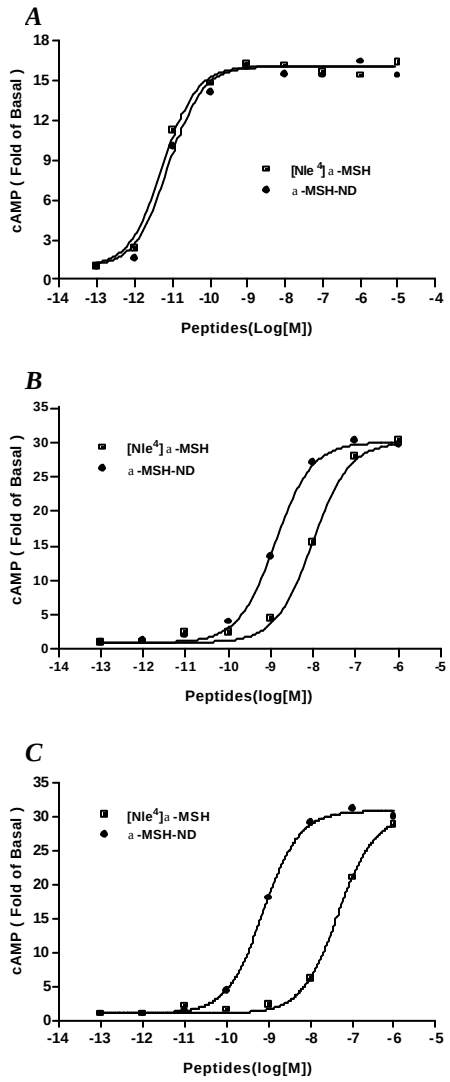


**Figure 6**. Measurement of intracellular cAMP in response to increasing concentration of the α-MSH analogues ([Nle$^4$] α-MSH and α-MSH-ND) in CHO cell lines stably transfected with MC1R( **A**), MC3R(**B**) and MC4R(**C**). Each experiment was performed in triplicate and repeated twice.

Being identical to the binding assay results described above, [Nle$^4$]α-MSH also exhibited a better cAMP-generating activity than α-MSH-ND at MC1R (Figure 6A). It is noteworthy that, for MC3R and MC4R, α-MSH-ND exhibited relatively higher activity than [Nle$^4$]α-MSH at the two receptors (Figure 6B and 6C). Compared with their cAMP stimulation at MC3 and MC4R, the two analogues showed the higher biological activities at MC1R, which was in keeping with the results shown in the binding assay.

Figure 7 showed the cAMP-generating activity of the substitutes which 6$^{th}$ residues were exchanged instead of His$^6$. At MC1R, they displayed the biological activity with the order of α-MSH-ND >> [Arg$^6$]α-MSH-ND > [Lys$^6$]α-MSH-ND > [Asn$^6$]α-MSH-ND > [Gln$^6$]α-MSH-ND > [Tyr$^6$]α-MSH-ND > [Trp$^6$]α-MSH-ND (Figure 7A). At MC3R, [Arg$^6$]α-MSH-ND exhibited a higher

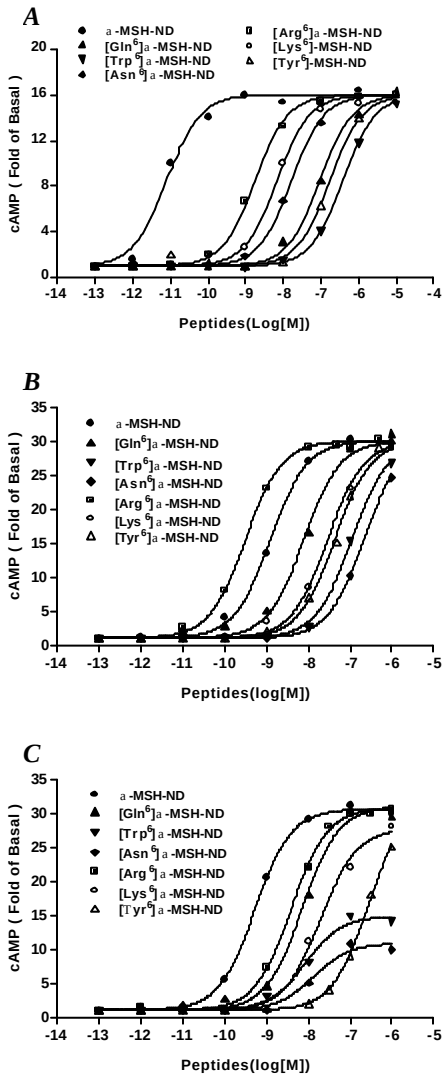


**Figure 7.** Measurement of intracellular cAMP in response to increasing concentration of the α-MSH analogues (α-MSH-ND, [Gln$^6$]α-MSH-ND, [Trp$^6$]α-MSH-ND, [Asn$^6$]α-MSH-ND, [Arg$^6$]α-MSH-ND, [Lys$^6$]α-MSH-ND and [Tyr$^6$]α-MSH-ND) in CHO cell lines stably transfected with MC1R( **A**), MC3R(**B**) and MC4R(**C**). Each experiment was performed in triplicate and repeated twice.

receptor-binding results. Here, [Asn$^6$]α-MSH-ND and [Trp$^6$]α-MSH-ND displayed the weakest cAMP generating activity of all these peptides at MC3R, potency than α-MSH-ND, which was different from the binding assay data shown above, while still being lower than α-MSH-ND at the MC4R (Figure 7C), which was also identical to the

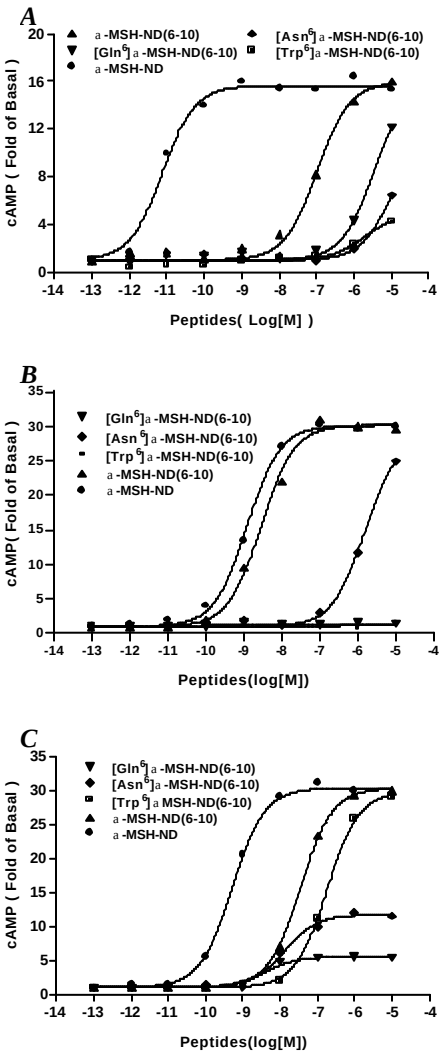


**Figure 8.** Measurement of intracellular cAMP in response to increasing concentration of the α-MSH analogues (α-MSH-ND, α-MSH-ND(6-10), [Gln$^6$]α-MSH-ND(6-10), [Asn$^6$]α-MSH-ND(6-10) and [Trp$^6$]α-MSH-ND(6-10) ) in CHO cell lines stably transfected with MC1R( **A**), MC3R(**B**) and MC4R(**C**). Each experiment was performed in triplicate and repeated twice.

while being incapable of generating the maximum cAMP response at the MC4R like the other peptides (Figure 7B). The potency order of all these peptides was [Arg$^6$]α-MSH-ND > α-MSH-ND > [Gln$^6$]α-MSH-ND > [Lys$^6$]α-MSH-ND > [Trp$^6$]α-MSH-ND > [Asn$^6$]α-MSH-ND at the MC3R (Figure 7B); and α-MSH-ND > [Arg$^6$]α-MSH-ND > [Gln$^6$]α-MSH-ND > [Lys$^6$]α-MSH-ND > [Tyr$^6$]α-MSH-ND > [Trp$^6$]α-MSH-ND ≈ [Asn$^6$]α-MSH-ND at MC4R (Figure 7C). With comparing the potency of these analogues, substitution of His$^6$ by other residues induced the most significant decrease of the activity in MC1R.

**Table 3.** $EC_{50}$ Values (mean±SEM) of MSH analogues obtained from computer analysis of dose-response curves on stable transfected CHO Cells over-expressing MC1R, MC3R or MC4R. The values underlined in Italics mean that their mature cAMP failed to reach the maximum stimulation as shown by other analogues; —, The compounds did not show the visible effect on cAMP-generation even at the highest concentration ($10^{-5}$M)

| Ligands | $EC_{50}$(nM) | | |
|---|---|---|---|
| | MC1R | MC3R | MC4R |
| [Nle$^4$]α-MSH | 0.00558 ± 0.00131 | 9.362 ± 1.932 | 46.040 ± 0.020 |
| α-MSH-ND | 0.00799 ± 0.00451 | 1.523 ± 0.707 | 0.780 ± 0.405 |
| [Gln$^6$]α-MSH-ND | 96.62 ± 32.276 | 9.383 ± 4.620 | 7.880 ± 1.818 |
| [Trp$^6$]α-MSH-ND | 387.9 ± 164.10 | 110.00 ± 35.701 | *0.812 ± 0.428* |
| [Asn$^6$]α-MSH-ND | 16.77 ± 6.944 | 271.80 ± 21.948 | *0.799 ± 0.121* |
| [Arg$^6$]α-MSH-ND | 1.765 ± 0.800 | 0.381 ± 0.157 | 4.858 ±0.949 |
| [Lys$^6$]α-MSH-ND | 6.879 ± 2.650 | 29.560 ± 11.525 | 19.890 ± 4.024 |
| [Tyr$^6$]α-MSH-ND | 178.8 ± 45.269 | 76.860 ± 12.088 | 273.60 ± 259.668 |
| α-MSH-ND(6-10) | 104.30 ± 27.46 | 29.560 ± 5.260 | 40.050 ± 15.272 |
| [Gln$^6$]α-MSH-ND(6-10) | 3352 ± 1519 | — | *6.181 ± 5.327* |
| [Asn$^6$]α-MSH-ND(6-10) | 11640 ± 2910 | 5407.0 ± 2981.5 | *7.609 ± 6.133* |
| [Trp$^6$]α-MSH-ND(6-10) | *1795 ± 189* | — | 184.80 ± 110.625 |

α-MSH-ND(6-10), as seen in Figure 8A, showed the significantly lower activity than that of α-MSH-ND at MC1R. In MC3R and MC4R, α-MSH-ND(6-10) gave a comparatively good cAMP response, especially at the MC3R (Figure 8B). Substitutions of His$^6$ by Gln, Trp or Asn resulted in more decrease in their ability to stimulate cAMP formation. In particular, His$^6$/Asn$^6$ exchange led almost to a loss of all its biological activity at MC1R and MC4R (Figure 8A and 8C). Furthermore, His$^6$/Gln$^6$ exchange gave rise to absolute loss of its activity at MC3R and MC4R, while His$^6$/Trp$^6$ exchange almost resulted in complete disappearing of the activity at MC1R and MC3R. The $EC_{50}$ values of all the

analogues tested in this study are shown in Table 3.

**4. Solution structures of** a **-MSH analogues analyzed with NMR assay**

Using the experimental constraints from NMR data, sixteen-thirty structures of these α-MSH analogues were calculated by DG (distance geometry) followed by SA (simulated-annealing) method. Most of the backbone conformations are superimposed from $Asp^5$ to $Arg^8$. As shown in Figure 9, [$Nle^4$]α-MSH forms a hair pin loop conformation, whereas α-MSH-ND, a linear form of MTII, prefers a type I β-turn comprising residues $Asp^5$-$His^6$-(D-Phe)$^7$-$Arg^8$. In addition, the quality of the final structures of [$Gln^6$]α-MSH-ND, [$Gln^6$]α-MSH-ND(6-10) and [$Lys^6$]α-MSH-ND were also estimated. As seen in Figure 10A, [$Gln^6$]α-MSH-ND has a propensity to form a type I' β-turn, which is a mirror image corresponding to a type I β-turn around $Asp^5$-$Gln^6$-(D-Phe)$^7$-$Arg^8$. At the same time, [$Gln^6$]α-MSH-ND(6-10) adopted a γ-turn conformation composed with three residues of $Gln^6$-(D-Phe)$^7$-$Arg^8$ (Figure 10B). For [$Lys^6$]α-MSH-ND, a turn conformation appeared comprising the residues of $Asp^5$-$Lys^6$-D$Phe^7$-$Arg^8$. The peptide formed a right angle twist to make a bend conformation. This conformation distorted the orientation of $Asp^5$ and resulted in the weak hydrogen

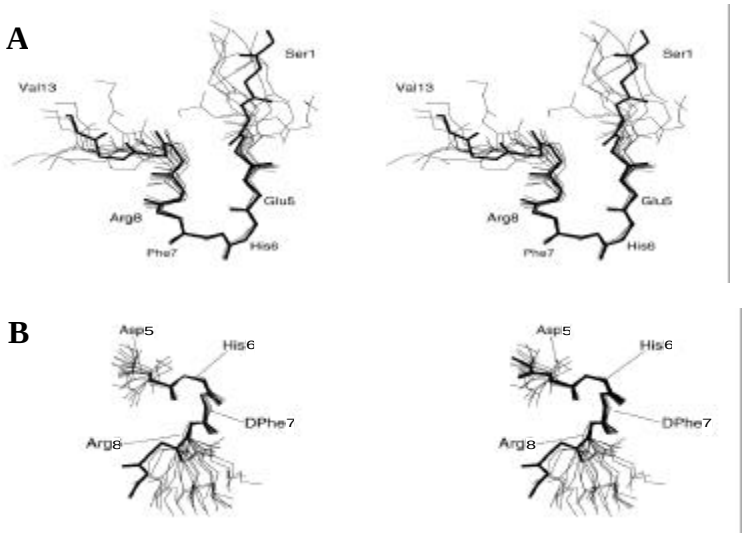


**Figure 9**. NMR structure of [$Nle^4$]α-MSH and α-MSH-ND. [$Nle^4$]α-MSH forms a hair pin loop conformation(**A**), whereas α-MSH-ND, a linear form of MTII, prefers a type I β-turn conprising residues $Asp^5$-$His^6$-(D-Phe)$^7$-$Arg^8$(**B**).

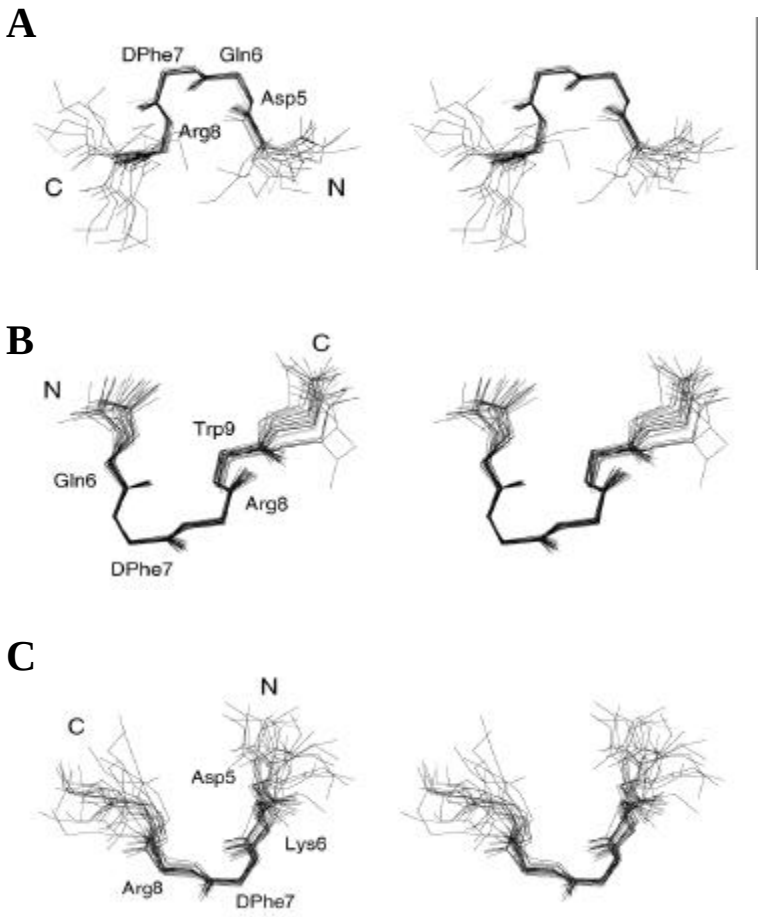


**Figure 10**. Final simulated-annealing structures of [Gln$^6$]α-MSH-ND (**A**), [Gln$^6$]α-MSH-ND(6-10) (**B**) and [Lys$^6$]α-MSH-ND (**C**). Superposition of the final structures(16, 27 and 21 structures for [Gln$^6$]α-MSH-ND, [Gln$^6$]α-MSH-ND(6-10) and [Lys$^6$]α-MSH-ND, respectively) displayed in stereoview. All backbone atoms of three α-MSH analogues are superimposed from Asp$^5$ to Arg$^8$ except for [Gln$^6$]α-MSH-ND(6-10) (from Gln$^6$ to Arg$^8$).

bond between the carbonyl oxygen of Asp$^5$ and amide hydrogen of Arg$^8$. This resulted in the lack of inter residue NOEs (rotating-frame Overhauser effect) as well as a stable hydrogen bond which are critical for β-turn formation. From hese data, the REM (restraint-energy minimization) structure of [Lys$^6$]α-MSH-ND demonstrated a γ-turn conformation around Lys$^6$-(D-Phe)$^7$-Arg$^8$ (Figure10C).

It is interesting that [Gln$^6$]α-MSH-ND exhibited a similar backbone structure to α-MSH-ND. As shown in Figure 11, the REM structure of α-MSH-ND and [Gln$^6$]α-MSH-ND was superimposed with respect to the residues from Asp$^5$ to

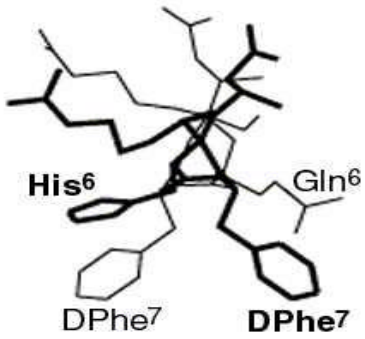


**Figure 11. Conformational difference of α-MSH-ND and [Gln$^6$]α-MSH-ND.** It shows the superposition of the backbone conformations for the α-MSH-ND (thick line) and [Gln$^6$]α-MSH-ND (thin line) structures. Backbone structure of [Gln$^6$]α-MSH-ND is aligned for residues Asp$^5$-Arg$^8$ of α-MSH-ND.

Arg$^8$ of α-MSH-ND. The solution structures of α-MSH-ND and [Gln$^6$]α-MSH-ND are aligned for primary sequences so that the corresponding residues of the peptides are located in the same orientation. It was found that the side chains of the center residues of the β-turn, His$^6$ and D-Phe$^7$ at α-MSH-ND or Gln$^6$ and D-Phe$^7$ at [Gln$^6$] α-MSH-ND, have the opposite direction, whereas, the orientations of Arg$^8$ and Trp$^9$ are similar. This demonstrates that the 6$^{th}$ and 7$^{th}$ residues of [Gln$^6$]α-MSH-ND have a mirror image conformation relative to α-MSH-ND.

**4. Evaluation of receptor-ligand interaction patterns by homology modeling**

In our model, polar side chain of His$^6$ in α-MSH-ND was found to interact with TM2 domains of the three MC receptors, which were Glu$^{94}$ of MC1R, Glu$^{94}$ of MC3R and Glu$^{100}$ of MC4R, respectively (Figure 12). At the same time, the residue of Arg$^8$ of this ligand bound to residues of TM3 domains including Asp$^{121}$ in MC1R, Asp$^{121}$ in MC3R and Asp$^{126}$ in MC4R, respectively. With the exchange of 6$^{th}$ residue from His to Gln, [Gln$^6$]α-MSH-ND showed a mirror image corresponding to α-MSH-ND with changed orientations of the 6$^{th}$ and 7$^{th}$ residues. Since the direction of side chain of the Gln$^6$ residue was different from that of the His$^6$ residue, the side chain of Gln$^6$ could not bind to the TM2 domains of all the receptors, whereas the Arg$^8$ and Trp$^9$ residue of [Gln$^6$]α-MSH-ND maintain the interaction same as α-MSH-ND.

Phenyl ring of α-MSH-ND interacted with Cys$^{275}$ and Ile$^{276}$ of MC1R, Cys$^{276}$ and Tyr$^{277}$ of MC3R, or Cys$^{279}$ and Phe$^{280}$ of MC4R that belongs to TM7 region of each receptor. However, D-Phe$^7$ of [Gln$^6$]α-MSH-ND could not have contact with these residues. Instead, it would adjoin to the residues of TM3 domains,

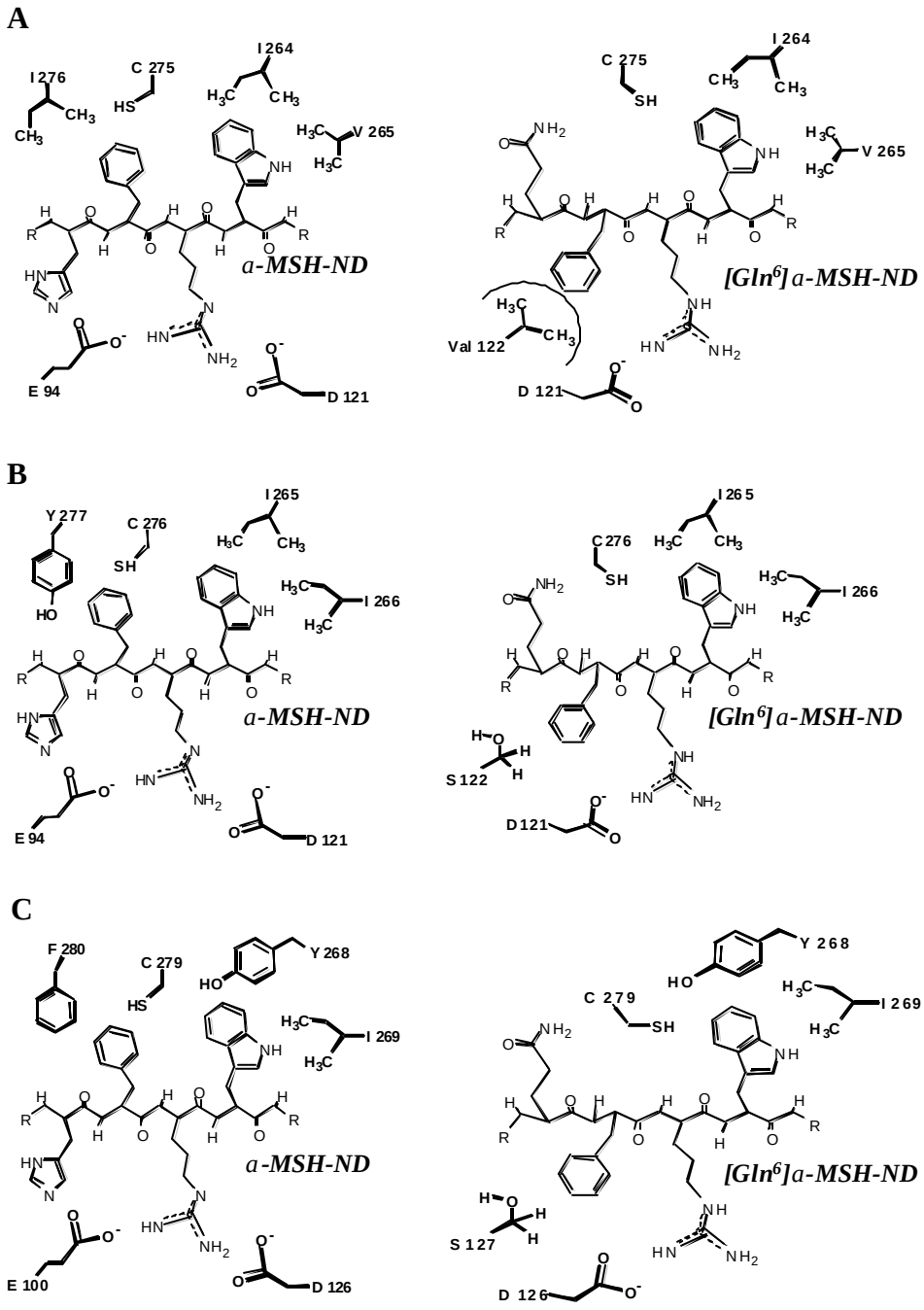


**Figure 12. Schematic Diagram of Ligand-Receptor Binding Model.** Possible interactions between ligands and receptors are delined from the complex structures based on NMR structures of ligands and homology models of receptors for MC1R(**A**), MC3R(**B**) and MC4R(**C**). Structures of both α-MSH-ND and [Gln6]α-MSH-ND are displayed with thin lines whereas residues from receptors are displyed with thick lines.

$Ser^{122}$ of MC3R or $Ser^{127}$ of MC4R (Figure 12B and 12C). The residues with polar side chain are oriented to the opposite direction of TM7 binding site. In MC1R, these serine residues correspond to $Val^{122}$ that contains the non-polar side chain including two methyl groups (Figure 12A). It was noteworthy that the important residues in the hydrophobic binding pockets of MC1R were different. The $Ile^{276}$ residue of MC1R, which is involved in D-$Phe^{7}$ binding site, was changed to $Tyr^{277}$ in MC3R and $Phe^{280}$ in MC4R. On the other hand, the residues of each receptor at $Trp^{9}$ binding cavity lying in TM6 domains, $Ile^{264}$ of MC1R or $Ile^{265}$ of MC3R were replaced with $Tyr^{268}$ in MC4R. $Val^{265}$ in MC1R, the other residue interacting with $Trp^{9}$, was substituted with $Ile^{266}$ in MC3R and $Ile^{269}$ in MC4R. Our models indicated that TM2, TM3, TM6 and TM7 segments of receptors would participate in the formation of the binding pocket for the core sequence of α-MSH analogues. These structures are well supported by the mutagenesis studies clarifying that TM4 and TM5 are not involved in the binding pocket(52).

**6. Feeding Assay in Normal Mice.**

In this study, it was found that α-MSH-ND showed the best biological

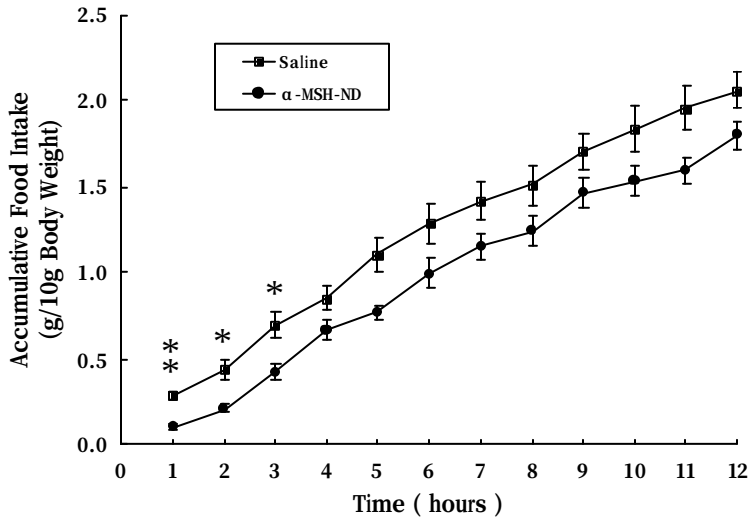


**Figure 13**. **Effect of intraperitoneal administration of** a**-MSH-ND on feeding in ICR mice** (male, 25-30 g). Mice were fasted over night. Animals received 100 nmole of α-MSH-ND, or an equal volume (100 μl) of saline alone. Data points indicate the mean values of accumulative food intake amounts, bars indicating their standard error. Significance indicated for individual time points. * $P<0.05$, ** $P<0.01$, 100 nmole of α-MSH-ND versus saline.

activity of all synthetic melanocortin analogues. Therefore, the effect of α-MSH-ND on food intake was studied in 20-30 g normal male ICR mice. Compared to vehicle (saline)-injected mice, intraperitoneal injection of α-MSH-ND (100 nmole) caused a significant inhibition of feeding within the first one hour ($P < 0.01$, Figure 13). The inhibitory effect lasted for up to 3 hours after administration ($P < 0.05$). After 3 hours, the food intake of α-MSH-ND-treated group entered normal rates consuming.

# IV. DISCUSSION

With the cloning of the melanocortin receptors, the molecular mechanisms underlying a variety of effects have started to become elucidated. It is now clear that most, if not all, of the effects of the melanocortin peptides are mediated via specific subtypes of melanocortin receptors[16]. Some of the new findings indicate that melanocortin receptors may serve as targets for novel drugs. For instance, MC3R and MC4R, unlike the other melanocortin subtypes, were found mainly at distinct loci in the central nervous system, such as the ventromedial nucleus of the hypothalamus (VMH), which is considered most important in the regulation of feeding behavior and lesions of the VMH, are associated with an increase in body weight. Recent reports with knockout techniques[34,53,54] and i.c.v. injection of the cyclic MSH analogues SHU9119 and MTII[6] linked the MC3R and MC4R to feeding behavior and weight homeostasis.

All of the natural melanocortins contain the conserved core structure (i.e., $His^6$-$Phe^7$-$Arg^8$-$Trp^9$), and each of the core residues has been thought to exhibit an important effect for biological activity[2,55-57]. From this study, it was found that, although being free of six N- and C-terminal amino acid residues, α-MSH-ND (a linear form of MTII) revealed a higher binding affinity and cAMP-generating activity at MC3R and MC4R. In contrast, [$Nle^4$]α-MSH showed a better potency at MC1R. In the NMR study, [$Nle^4$]α-MSH revealed a loop structure, while α-MSH-ND exhibiting a "type I β-turn" structure. These results indicate that type I β-turn is important for augmenting biological activity in

MC3R and MC4R. Compared to [Nle$^4$]α-MSH, α-MSH-ND exhibited the relatively weak potency at MC1R, which suggest that the N- and C-terminal residues of [Nle$^4$]α-MSH are also important for enhancing the potency of ligands to MC1R.

To further investigate the role of type I β-turn as well as the 6$^{th}$ residue in activation of melanocortin receptors, we changed the His$^6$ residue of α-MSH-ND by Gln, Trp, Asn, Arg, Lys or Tyr and examined their biological activity. Substitution of His$^6$ residue of α-MSH-ND by Gln, Trp, Asn, Lys or Tyr resulted in remarkable reduction of their biological activity. Compared to MC3R and MC4R, most of the α-MSH analogues except [Arg$^6$]α-MSH-ND exhibited more significant decrease in their binding affinity to MC1R. With regard to cAMP-generating activity, those analogues containing positive charged residue at the 6$^{th}$ position, such as α-MSH-ND, [Arg$^6$]α-MSH-ND and [Lys$^6$]α-MSH-ND, showed relatively high cAMP-generating activity at MC3R and MC4R. These results suggest that, firstly, the 6$^{th}$ residue would play an important role in the activation of the three receptor subtypes, and secondly, there could be some charge interaction between the 6$^{th}$ residue of α-MSH-ND and the receptors even though the effect is likely not critical for some subtypes. However, at all of the receptors, [Lys$^6$]α-MSH-ND showed a significantly lower binding affinity than [Arg$^6$]α-MSH-ND. From the NMR study, [Lys$^6$]α-MSH-ND demonstrated a γ-turn like conformation around Lys$^6$-(D-Phe)$^7$-Arg$^8$. This suggests that, for the two analogues, the different potencies were probably the result of the distinct size of their sixth residues rather than the electrical charge.

Except the binding affinity of [Trp$^6$]α-MSH-ND(6-10) for MC1R, truncation of Nle$^4$ and Asp$^5$ of α-MSH-ND remarkably decreased the receptor-binding and cAMP-generating activity at all receptors. [Gln$^6$]α-MSH-ND(6-10) was almost unable to activate all the receptors, even though it could bind to these receptors. In the NMR study, although [Gln$^6$]α-MSH-ND(6-10) is composed of only five amino acid residues, it revealed a very stable structure, a tight γ-turn composed of Gln$^6$-(D-Phe)$^7$-Arg$^8$. Therefore, a plausible explanation for the remarkable loss of

the receptor-binding and cAMP-generating activity of the truncated analogues might be that these short analogues could no longer maintain a stable classic type I β-turn conformation. On the other hand, α-MSH-ND(6-10) was able to generate the maximum stimulation of the receptors at the higher concentration, whereas, [Gln$^6$]α-MSH-ND(6-10) was almost completely incapable of stimulating both receptors. This suggests that the degree of flexibility and ability of truncated analogues for receptor activation might be partially dependent on the flexible free N-terminal end of the 6$^{th}$ residue itself. In combination with the NMR results of [Lys$^6$]α-MSH-ND and [Gln$^6$]α-MSH-ND(6-10), they also suggest that the more the structure of an α-MSH-ND-derived analogue diverges from the type I β-turn, the less its biological activity at these receptors.

However, a very interesting finding in this study is that, α-MSH-ND revealed a tight type I β-turn conformation, while [Gln$^6$]α-MSH-ND showing a type I' β-turn structure, a very similar structure to that of α-MSH-ND. Despite this subtle difference in back bone structures between the two oligopeptides, [Gln$^6$]α-MSH-ND gave the significant lower biological activity than α-MSH-ND. In particular, compared to MC3R and MC4R, [Gln$^6$]α-MSH-ND exhibited an approximate 10,000-fold less biological activity than α-MSH-ND at MC1R. From the NMR analysis, it was found that the backbone structures of α-MSH-ND and [Gln$^6$]α-MSH-ND are very similar, whereas their side chain orientations are quite different, and [Gln$^6$]α-MSH-ND is a mirror image analogue of α-MSH-ND. To define how such conformational differences result in such great differences in the biological activity at MC1R, we compared their individual binding patterns to these receptors. Molecular modeling analysis revealed that the positively charged His$^6$ residue of α-MSH-ND interacts with the negatively charged glutamine residues in the TM2 regions of the three melanocortin receptors, whereas Gln$^6$ of [Gln$^6$]α-MSH-ND does not. This indicated that the changed side chain orientation of the latter and its lack of a charge interaction with the TM2 regions are responsible for the significant loss of biological activity at these receptors. Hydrophobic binding pockets in each receptor were composed

of diverse hydrophobic amino acids, which may also confer binding activity or specificity. NMR analysis showed that the D-Phe$^7$ residue of [Gln$^6$]α-MSH-ND orientated as the mirror image of the corresponding α-MSH-ND position. This directional displacement changed the D-Phe$^7$ binding sites of all receptors from the hydrophobic binding domain of TM7 to TM3 regions as described in Figure 12. Therefore, the altered receptor-binding patterns of the D-Phe$^7$ residues of [Gln$^6$]α-MSH-ND could also explain its decreased biological potency at all receptors.

The TM2 regions of all the three receptor subtypes would not bind to [Gln$^6$]α-MSH-ND, as described above, because of the altered orientation of Gln$^6$, and the Arg$^8$- and Trp$^9$-binding sites of all three receptors did not exhibit obvious changes from one another. Therefore, the changed D-Phe$^7$ orientation in [Gln$^6$]α-MSH-ND was considered to be likely to be responsible for the significant decrease in biological activity at MC1R, while such a change was tolerable to MC3R and MC4R. As we expected, D-Phe$^7$ of [Gln$^6$]α-MSH-ND could not contact the hydrophobic binding region of TM7, as observed in α-MSH-ND, instead, it would adjoin to the residues of the TM3 domains in all of the three receptors. Compared to the changed binding sites of MC3R (Ser$^{122}$) and MC4R (Ser$^{127}$), it could be seen that, in MC1R, these serine residues correspond to Val$^{122}$, which contains two methyl groups. Since the phenyl ring of [Gln$^6$]α-MSH-ND coincidentally overlaps with these two bulky groups, we speculate that its interaction with the valine residue of MC1R, instead of the serine residue of MC3R or MC4R, induces steric hindrance with D-Phe$^7$ of the ligand, and that specifically the repulsion between these two residues results in the relatively low affinity of [Gln$^6$]α-MSH-ND to MC1R.

Among the synthetic α-MSH analogues, α-MSH-ND exhibited the most potent biological activity of all the synthetic analogues at MC3R and MC4R, which activity is comparable to that of a well known analogue, MTII (Ac-Nle-cyclic[Asp-His-DPhe-Arg-Trp-Lys]-$NH_2$)[58]. MTII has been reported to inhibit food intake in mice after administration intracerebroventricularly or

intraperitoneally at moderate dose[6]. Therefore, α-MSH-ND was tested to evaluate if it has inhibitory effect on food intake after intraperitoneal injection. Administration of α-MSH-ND significantly inhibited food intake of mice within 3 hours. This indicates that melanocortic peptides is associated directly with regulation of food intake, and that α-MSH analogues, especially those with high biological activity at MC3R and MC4R, could directly inhibit food intake. It also demonstrates indirectly that α-MSH-ND could penetrate the brain-blood barrier and modulate the region of central nervous system devolved in food intake.

The melanocortin receptors belong to the G-protein coupled receptor family, and all of them couple not only in the stimulatory fashion to cAMP, but also in other signal transduction system, including $IP_3$ pathway. In this study, the biological activities of α-MSH analogues were evaluated only by radio-ligand binding and cAMP-generation assays. To understand more detailed mechanisms of how melanocortins exert their different physiologic effects, further *in vitro* and *in vivo* studies of melanocortin analogues are required to investigate how they influence the other signal transduction pathway and what physiological effects they could bring on after acting on different melanocortin receptor subtypes.

# V. CONCLUSION

Taken together, the results obtained in this study suggest that type I β-turn conformation comprising the residues of $Asp^5$-$His^6$-(D-Phe)$^7$-$Arg^8$ is important, and the side chain orientations of $6^{th}$ and $7^{th}$ residues is critical for determination of potency and selectivity of melanocortin analogues. In addition, we demonstrated that minimization of MC1R with the preservation of comparable MC3R and MC4R selectivity could be achieved by modifying the D-$Phe^7$ orientation of α-MSH-ND, while keeping the 'type I β-turn'-like structure.

# REFERENCES


1. De Wied D, Jolles J. Neuropeptides derived from pro-opiomelanocortin: Behavioral, physiological and neurochemical effects. Physiol Rev 1982; 62: 976-1059.
2. Eberle AN. The Melanotropin: Chemistry, Physiology and Mechanisms of Action. Karger, Basle; 1988; pp: 149-319.
3. Simpson ER, Waterman MR. Regulation of the synthesis of steroidogenic enzymes in adrenal cortical cells by ACTH. Ann Rev Physiol 1988; 50: 427-440.
4. Ceriani G, Macalus A, Catania A, Lipton JM. Central neurogenic antiinflammatory action of α-MSH. Neuroendocrinol 1994; 59: 138-143.
5. Van Bergen P, Janssen PM, Hoogerhout P, De Wildt DJ, Versteeg DH. Cardiovascular effects of γ-MSH/ACTH-like peptides: structure-activity relationship. Eur J Pharmacol 1995; 294: 795-803.
6. Fan W, Boston BA, Kesterson RA, Hruby VJ, Cone RD. Role of melanocortinergic neurons in feeding and the agouti obesity syndrome. Nature 1997; 385: 165-168.
7. Contreras PC, Takemori AE. Antagonism of morphine-induced analgesia, tolerance and dependence by α-MSH. J Pharmacol Exp Ther 1984; 229: 21-26.
8. Smith EM, Hughes TK, Hashemi F, Stefano GB. Immunosuppressive effects of corticotropin and melanotropin and their possible significance in human immunodeficiency virus infection. Proc Natl Acad Sci USA 1992; 89: 782-786.
9. O'Donahue TL, Dorsa DM. The opiomelanotropinergic neuronal and endocrine systems. Peptides 1982; 3: 353-395.
10. Chhajlani V, Muceniece R, Wikberg JES. Molecular cloning and expression of the human melanocyte stimulating hormone receptor. Biochem Biophys Res Commun 1993; 195: 866-873.
11. Chhajlani V, Wikberg JES. The cloning of a family of genes that encode the melanocortin receptors. FEBS Lett 1992; 309: 417-420.
12. Gantz I, Konda Y, Tashiro T, Shimoto Y, Miwa H, Munzert G, et al. Molecular cloning of a novel melanocortin receptor. J Biol Chem 1993; 268: 8246-8250.
13. Gantz I, Miwa H, Konda Y, Shimoto Y, Tashiro T, Watson SJ, et al. Molecular cloning, expression and gene localization of a fourth melanocortin receptor. J Biol Chem 1993; 268: 15174-15179.
14. Mountjoy KG, Robbins LS, Mortrud TT, Cone RD. The cloning of a family

of genes that encode the melanocortin receptors. Science 1992; 257: 1248-1251.

15. Mountjoy KG, Wong J. Obesity, diabetes and functions for pro-opiomelanocortin-derived peptides. Mol Cell Endocrinol 1997; 128: 171-177.

16. Wikberg JES. Melanocortin receptors: perspectives for novel drugs. Eur J Pharmacol 1999; 375: 295-310.

17. Cone RD, Lu D, Koppula S, Vage DI, Klungland H, Boston B, et al. The melanocortin receptors: agonists, antagonists, and the hormonal control of pigmentation. Recent Prog Horm Res 1996; 51: 287-317.

18. Xia Y, Skoog V, Muceniece R, Chhajlani V, Wikberg JES. Polyclonal antibodies against human melanocortin MC1 receptor: preliminary immunohistochemical localisation of melanocortin MC1 receptor to malignant melanoma cells. Eur J Pharmacol 1995; 288: 277-283.

19. Star RA, Rajora N, Huang J, Stock RC, Catania A, Lipton JM. Evidence of autocrine modulation of macrophage nitric oxide synthase by α-melanocyte-stimulating hormone. Pro Natl Acad Sci USA 1995; 92: 8016-8020.

20. Hartmeyer M, Scholzen T, Becher E, Bhardwaj RS, Schwartz T, Luger TA. Human dermal microvascular endothelial cells express the melanocortin receptor type 1 and produce levels of IL-8 upon stimulation with alpha-melanocyte-stimulating hormone. J Immunol 1997; 159: 1930-1397.

21. Catania A, Rajora A., Capsoni F, Minonzio F, Star RA, Lipton JM. The neuropeptide α-MSH has specific receptors on neutrophils and reduces chemotaxis in vitro. Peptides 1996; 17: 675-679.

22. Wong KY, Rajora,N, Boccoli G, Lipton JM. A potential mechanism of local anti-inflammatory action of alpha-melanocyte-stimulating hormone within the brain: modulation of tumor necrosis factor-alpha production by human astrocytic cells. Neuroimmunomodulation 1997; 4: 37-41.

23. Boston BA, Cone RD. Characterization of melanocortin receptor subtype expression in murine adipose tissues and in the 3T3-L1 cell line. Endocrinology 1996; 137: 2043-2050.

24. Luger TA, Scholzen T, Grabbe S. The role of alpha-melanocyte-stimulating hormone in cutaneous biology. J Invest Dermatol Symp Proc 1997; 2: 87-93.

25. Roselli-Rehfuss L, Mountjoy KG, Robbins LS, Mortrud MT, Low MJ, Tatro JB, et al. Identification of a receptor for γ-melanotropin and other proopiomelanocortin peptides in the hypothalamus and limbic system. Proc Natl Acad Sci USA 1993; 90: 8856-8860.

26. Chhajlani V. Distrubution of cDNA for melanocortin receptor subtypes in

human tissues. Biochem. Mol Biol Int 1996; 38: 73-80.

27. Mountjoy KG, Mortrud MT, Low MJ, Simerly RB, Cone RD. Localization of the melanocortin-4 receptor (MC4-R) in neuroendocrine and autonomic control circuits in the brain. Mol Endocrinol 1994; 8: 1298-1308.

28. Takeuchi S, Takahashi S. Melanocortin receptor genes in the chicken-tissue distributions. Gen Comp Endocrinol 1998; 112: 220-231.

29. Woods SC, Seeley RJ, Porte JRD, Schwartz MW. Signals that regulated food intake and energy homeostasis. Science 1998; 280: 1378-1383.

30. Campfield LA, Smith FJ, Burn P. Strategies and potential molecular targets for obesity treatment. Science 1998: 280: 1383-1387.

31. Krude H, Bieberann H, Luck W, Hom R, Brabant G, Gruters A. Severe early-onset obesity, adrenal insufficiency and red hair pigmentation caused by POMC mutation in humans. Nature Genetics 1998; 19(2): 155-157.

32. Huszar D, Lynch CA, Fairchild-Huntress V, Dunmore JH, Fang Q, Berkemeier LR, et al. Targeted disruption of the melanocortin-4 receptor results in obesity in mice. Cell 1997; 88: 131-141.

33. Bultman SJ, Michaud EJ, Woychik RP. Molecular characterization of the mouse agouti locus. Cell 1992; 71(7): 1195-1204.

34. Chen AS, Marsh DJ, Trumbauer ME, Frazier EG, Guan XM, Yu H, et al. Inactivation of the mouse melanocortin-3 receptor results in increased fat mass and reduced lean body mass. Nature Genetics 2000; 26: 97-102.

35. Hadley ME, Marwan MM, Al-Obeidi F, Hruby VJ, Castrucci AM. Linear and cyclic alpha-melanotropin(4-10)-fragment analogues that exhibit superpotency and residual activity. Pigment Cell Res 1989; 2: 478-484.

36. Hruby VJ, Lu D, Sharma SD, Castrucci A DeL, Kesterson RA, Al-Obeidi FA, et al. Cyclic lactam α-melanotropin analogues of Ac-Nle$^4$-cyclo[Asp$^5$, D-Phe$^7$, Lys$^{10}$]α-melanocyte-stimulating hormone-(4-10)-$NH_2$ with bulky aromtic amino acids at position 7 show high antagoinst potency and selectivity at specific melanocortin receptors. J Med Chem 1995; 38: 3454-3461.

37. Schiöth HB, Muceniece R, Mutulis F, Prusis P, Lindeberg G, Sharma SD, et al. Selectivity of cyclic [D-Nal$^7$] and [D-Phe$^7$] substituted MSH analogues for the melanocortin receptor subtypes. Peptides 1997; 18(7): 1009-1013.

38. Sawyer TK, Sanfilippo PJ, Hruby VJ, Engel MH, Heward CB, Burnett JB, et al. 4-Norleucine, 7-D-pheylalanine-α-melanocyte-stimulating hormone: a highly potent alpha-melanotrophin with ultralong biological activity. Proc Natl Acad Sci USA 1980; 77(10): 5754-5758.

39. Schiöth HB, Muceniece R, Wikberg JE. Selectivity of [Phe-1$^7$], [Ala$^6$] and [D-Ala$^4$, Gln$^5$, Tyr$^6$] substituted ACTH(4-10) analogues for the melanocortin receptors. Peptides 1997; 18(5): 761-763.

40. Li SZ, Lee JH, Lee W, Yoon CJ, Baik JH, Lim SK. Type I β-turn is important for biological activity of the melanocyte-stimulating hormone analogues. Eur J Biochem 1999; 265: 430-440.

41. Davis DG, Bax A. Assignment of complex $^{1}H$ NMR spectra via two-dimensional homonuclear Hartmann-Hahn spectroscopy. J Am Chem Soc 1985; 107: 2820-2821.

42. Jeener J, Meier BH, Bachman P, Ernst RR. Investigation of exchange processes by two-dimensional NMR spectroscoopy. J Chem Phys 1979; 71: 4546-4553.

43. Rance M, Sorensen OW, Bodenhausen G, Wagner G, Ernst RR, Wuthrich K. Improved spectral resolution in COSY $^{1}H$-NMR spectra of proteins via double quantum filtering. Biochem Biophs Res Commun 1983; 117: 479-485.

44. Marion D, Wuthrich K. Application of phase sensitive two-dimensional correlated spectroscopy (COSY) for measurements of $^{1}H$-$^{1}H$ spin-spin coupling constants in proteins. Biochem Biophs Res Commun 1983; 113: 967-974.

45. Otting G, Widmer H, Wagner G, Wuthrich K. Origin of $t_1$ and $t_2$ ridges in 2D NMR spectra and procedures for suppression. J Magn Reson 1986; 66: 187-193.

46. Lee W, Moore CH, Watt DD, Krishna NR. Solution structure of the variant-3 neurotoxin from Centruroides sculpturatus Ewing. Eur J Biochem 1994; 218: 89-95.

47. Adan RAH, Gispen WH. Bran melanocoritin receptors: from cloning to function. Peptides. 1997; 18: 1279-1287.

48. Haskell-Luevano C, Hendrata S, North C, Sawyer TK, Hadley ME, Hruby VJ, et al. Discovery of prototype peptidomimetic agonists at the human melanocortin receptors MC1R and MC4R. J Med Chem 1997; 40: 2123-2129.

49. Baldwin JM, Schertler FXG, Unger VM. An alpha-carbon template for the transmembrane helices in the rhodopsin family of G-protein-coupled receptors. J Mol Biol 1997; 272: 144-164.

50. Prusis P, Frandberg,PA, Muceniece R, Kalvinsh I. A three dimensional model for the interaction of MSH with the melanocortin-1 receptor. Biochem Biophy Res Comm 1995; 210: 205-210.

51. Yang YK, Dickinson C, Haskell-Luvano C, Gantz I. Molecular basis for the interaction of [Nle$^{4}$, D-Phe$^{7}$]melanocyte-stimulating hormone with the human melanocortin-1 receptor. J Biol Chem 1997; 272: 23000-23010.

52. Schiöth HB, Muceniece R, Szardenings M, Prusis P, Wikberg JES. Evidence indicating that the TM4, EL2 and TM5 of the melanocortin 3 receptor do

not participate in ligand binding. Biochem Biophys Res Commun 1996; 229: 687-692.

53. Kask A, Rago L, Korrovits P, Wikberg JE, Schiöth HB. Evidence that orexigenic effects of melanocortin 4 receptor antagonist HS014 are mediated by neuropeptide Y. Biochem Biophys Res Commun 1998; 248(2): 245-249.

54. Kesterson RA, Huszar D, Lynch CA, Simerly RB, Cone RD. Induction of neuropeptide Y gene expression in the dorsal medial hypothalamic nucleus in two models of the agouti obesity syndrome. Mol Endocrinol 1997; 11(5): 630-637.

55. Schiöth HB, Muceniece R, Wikberg JES, Chhajlani V. Characterization of melanocortin receptor subtypes by radioligand binding analysis. Eur J Pharmcol 1995; 288(3): 311-317.

56. Schiöth HB, Muceniece R, Wikberg JE. Characterization of the melanocortin 4 receptor by radioligand binding. Pharmacol Toxicol 1996; 79(3): 161-165.

57. Schiöth HB, Muceniece R, Larsson M, Mutulis F, Szardenings M, Prusis P, et al. Binding of cyclic and linear MSH core peptides to the melanocortin receptor subtypes. Eur J Pharmcol 1997; 319: 369-373.

58. Al-Obeidi RAH, Hadley ME, Pettitt BM, Hruby VJ. Design of a new class of superpotent cyclic α-melanotropin based on quenched dynamic simulation. J Am Chem Soc 1989; 111: 3413-3416.

## 국문요약

# 멜라노코틴 유도체의 구조 및 기능에 관한 연구

멜라노코틴(melanocortin)은 색소침착, 부신피질 스테로이드 생합성, 기억, 혈압 및 체중 등의 조절에 관여하는 것으로 알려졌으며, 다섯 가지 멜라노코틴 수용체의 클로닝(cloning)은 멜라노코틴의 작용 기전을 연구 하는데 새로운 장을 열어주었다. MC3R 및 MC4R 효현제(agonist)는 현재 개발되고 있는 가장 중요한 비만치료제 후보물질중의 하나다. 그러나 특정 멜라노코틴 수용체 아형, 특히 MC3R 와 MC4R 에 대한 활성도가 크고 선택성(selectivity)이 높은 효현제는 아직 개발 되지 못하였다. 이에 연구자 등은 특정 멜라노코틴 수용체 아형에 대한 높은 역가(potency)와 선택성을 가진 유도체를 탐색하고, 멜라노코틴 및 그 수용체간의 상호작용의 특징을 보다 구체적으로 조사하고, 또 비만치료제로 쓰일 수 있는 후보 물질을 탐색하기 위하여 본 연구를 수행하였다. 먼저 hMC1R, rMC3R 및 hMC4R cDNA 를 CHO 세포에 영구적으로 도입(stable transfection) 시켜서 각 멜라노코틴 수용체 아형을 과 표현하는 세포주를 만들었다. 여러 가지 멜라노코틴 유도체를 합성한 후 각 멜라노코틴 수용체 아형에 대한 활성도를 radioligand-binding assay 및 cAMP-generating assay 방법으로 측정하였으며, 유도체들의 구조 및 유도체-수용체간의 결합 및 활성화 기전을 규명하기 위해서 NMR 과 homology modeling 방법을 도입 분석하였다. MC3R 및 MC4R 에서 α-MSH-ND 는 [Nle$^4$]α-MSH 에 비해 높은 활성도를 보였다. NMR 분석결과 α-MSH-ND 는 Type I β-turn 구조를 보인 반면에 [Nle$^4$]α-MSH 는 헤어핀 루프(hairpin loop) 구조를 보였다. α-MSH-ND 의 6 번째 His 을 다른 아미노산들로 치환할 때 [Arg$^6$]α-MSH-ND 를 제외하고는 세 가지 멜라노코틴 수용체 아형 모두에서 활성도가 현저하게 감소되었다. 한편 NMR 구조연구에서는 [Gln$^6$]α-MSH-ND 는 Type I′ β-turn 구조를 [Lys$^6$]α-

MSH-ND 및 [Gln$^6$]α-MSH-ND(6-10)는 γ-turn 구조를 보였다. 흥미롭게도 [Gln$^6$]α-MSH-ND 의 활성도는 α-MSH-ND 에 비해 MC3R 및 MC4R 에 대하여 약간 떨어지는 반면에 MC1R 에서 10,000 배 정도 감소되었다. Homology modeling 분석결과 유도체의 6 번째 아미노산기가 His 에서 Gln 로 치환함으로 6 번째 및 7 번째 아미노산기의 측쇄 방향(side chain orientation)이 α-MSH-ND 의 것과 서로 반대 방향으로 위치하는 것을 관찰 하였다. 따라서 수용체 결합부위(binding pocket)에 대한 유도체의 결합양상이 바뀐 것이 세 수용체 모두에서 두 유도체 활성도의 현저한 차이를 나타나는 원인인 것으로 사료된다. [Gln$^6$]α-MSH-ND 의 7 번째 아미노산기 D-Phe 의 phenyl ring 이 MC3R 및 MC4R 의 TM3 부위의 Ser$^{122}$ 및 Ser$^{127}$과 각각 결합하는 반면에 MC1R 에서 유도체의 D-Phe 과 결합하는 부위가 두개 큰 methyl group 를 가지고 있는 Val$^{122}$ 로 바뀌었다. 따라서 [Gln$^6$]α-MSH-ND 와 MC1R 의 결합은 MC3R 및 MC4R 에 결합하는 것보다 더 어려운 것으로 사료되었다. 한편 In vivo 실험에서 MC3R 및 MC4R 에 대한 활성도가 가장 높은 유도체인 α-MSH-ND 를 정상 수컷 ICR 백서 복강내에 투여한 결과 연속 3 시간동안의 식이섭취(food intake)가 현저하게 억제되는 것은 관찰 하였다. 결론적으로 멜라노코틴의 핵심 아미노산기(core residue)인 His$^6$-(D-Phe)$^7$-Arg$^8$-Trp$^9$ 의 His$^6$ 중심으로 한 type I β-turn 구조가 멜라노코틴 유도체의 활성도를 결정하는데 매우 중요한 것으로 사료되며 6 번째 및 7 번째 아미노산기의 측쇄 방향도 멜라노코틴의 활성도를 결정하는데 중요하다는 것을 알 수 있었다.

---

**핵심되는말:** 멜라노코틴 수용체, binding affinity, cAMP-generating activity, 핵자기 공명, type I β-turn, homology modeling